52 KSME Journal, Vol. 8, No. 1, pp. 52~62, 1994

Stress Singularities in Dissimilar Orthotropic Composites Containing an Interlaminar Crack

Hyung Jip Choi*

(Received June 11, 1993)

The problem of an interlaminar crack in dissimilar orthotropic composite materials under in-plane and anti-plane loading conditions is investigated. In the analytical model, orthotropic half-spaces are assumed to be bound together by a matrix interlayer which represents the matrix-rich interlaminar region in the fiber-reinforced composite laminate. The crack is embedded within the interlayer. With the utilization of the stiffness matrix approach, a system of singular integral equations of the first kind is derived for the current mixed boundary value problem. Numerical results are obtained for the interlaminar crack in a [0°/90°] fibrous composite laminate subjected to three basic loadings in fracture mechanics. Under each applied loading, variations of major and coupling stress intensity factors with respect to relative crack size, crack location, and fiber volume fraction are illustrated.

Key Words : Dissimilar Orthotropic Composite Materials, Interlaminar Crack, Matrix Interlayer, Stiffness Matrix Formulation, Singular Integral Equations, Stress Intensity Factors

1. Introduction

An issue of fundamental interest and technical importance in the area of stress analysis of layered media has been increasingly focused on the situation when such materials contain a crack. Caused by the material as well as geometric discontinuity, the near-tip behavior is rather complicated via the coupling among different modes of fracture even under a simple loading condition. Furthermore, the complex power singularity is attained for the crack located along the material interface, giving rise to the oscillatory crack-tip singular stress field with the ensuing controversial phenomenon of crack surface interpenetration. Specific solutions can be found in the work of England (1965), Erdogan and Gupta (1971), and Toya (1992), to name a few, for the problem of an interface crack in isotropic bimaterials. For the orthotropic counterpart, solutions are due to Sun and Manoharan (1989), Dhaliwal and Saxena (1990), and Hwu (1993). It was also illustrated by Sun and Manoharan (1989) and Toya (1992) that the respective modes of strain energy release rates for the interface crack do not converge in the conventional concept of crack closure integrals. As discussed by England (1965) and Atkinson (1977), however, such anomalous behavior is regarded to be inevitable for the linear elastic solutions to this class of crack problems, which are obtained based on the ideal interface modeling with zero thickness. On the other hand, Wu and Chiu (1991) showed that the anti-plane shear interface crack in both the isotropic and orthotropic bimaterials retains the usual square-root singularities. A further overview pertaining to this category of crack problems was reported by Rice (1988) and Comninou (1990).

Although the crack surface interference in a tensile field is a highly localized one confined to an extremely small region behind the crack tip, various refined models have been proposed to resolve the oscillatory behavior. For instance, Comninou (1977) assumed that crack surfaces in

* Power Engineering Research Institute, Korea Power Engineering Company, Inc. P.O. Box 631, Young-Dong Seoul, Korea

isotropic bimaterials are in frictionless contact close to the crack tip, while Sinclair (1980) and Itou (1986) represented the interface crack with a finite wedge angle. Atkinson (1977) and Delale and Erdogan (1988) suggested a diffusive interfacial layer as an alternative to the ideal interface. The frictionless contact model was later extended by Wang and Choi (1983) to the interface crack problem of dissimilar anisotropic materials.

In this paper, the stress analysis is performed for the in-plane and anti-plane problem of an interlaminar crack in dissimilar orthotropic composite materials. Based on the microscopic observation that delamination in the fiber-reinforced laminated composite is a matrix-dominated, progressive failure mechanism (Wang and Wang, 1979), the crack is embedded within a matrix interlayer bounded by the dissimilar orthotropic half-spaces. The interlayer models the matrix-rich interlaminar region of the fibrous composite laminate, which is also justifiable by the fact that layers of such composite laminates are usually bound together by the same matrix material in the constituent fibrous layers (Jones, 1975). The stiffness matrix method (Choi and Thangjitham, 1991a,b) is extended to formulate the current crack problem as a system of singular integral equations of the first kind. As numerical illustrations, the response of an interlaminar crack in a [0°/90°] laminated composite to in-plane normal, in-plane shear, and anti-plane shear loadings is presented in terms of major and coupling stress intensity factors. Under each applied loading, the effects of relative crack size, crack location, and fiber volume fraction are discussed.

2. Problem Definition and Formulation

Dissimilar orthotropic half-spaces bound together by a matrix-rich interlaminar region are considered. The interlaminar region is modeled in the form of an interlayer of uniform thickness $2h$ containing the crack of length 2a as shown in Fig. 1. As a result, the interlayer can be represented as two separate layers but with the identical isotropic matrix properties located above ($0<z<h_1$) and below ($-h_2<z<0$) the crack surface. The upper and lower half-spaces are then regarded to be fiber-reinforced along the x-($\theta=0°$) and y-directions ($\theta=90°$), respectively.

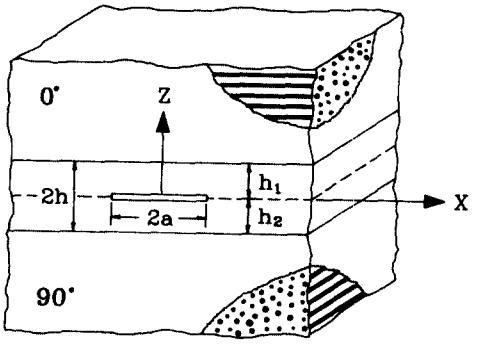

Fig. 1 Configuration of bonded dissimilar orthotropic half-spaces containing an interlaminar crack in a matrix interlayer

2.1 Governing Equations

Upon assuming that external loadings are applied such that the resulting field variables are independent of y-axis, the displacement field is written as

$$u=u(x, z),\ v=v(x, z),\ w=w(x, z) \qquad (1)$$

where u, v and w are the displacement components in the x-, y-, and z-directions, respectively, and the constitutive equations for orthotropic materials, in general, are given as (Lekhnitskii, 1981)

$$\begin{aligned}
\sigma_{xx}&=C_{11}\frac{\partial u}{\partial x}+C_{13}\frac{\partial w}{\partial z},\\
\sigma_{yy}&=C_{12}\frac{\partial u}{\partial x}+C_{23}\frac{\partial w}{\partial z},\\
\sigma_{zz}&=C_{13}\frac{\partial u}{\partial x}+C_{33}\frac{\partial w}{\partial z},\\
\tau_{yz}&=C_{44}\frac{\partial v}{\partial z},\\
\tau_{xz}&=C_{55}\left(\frac{\partial u}{\partial z}+\frac{\partial w}{\partial x}\right),\\
\tau_{xy}&=C_{66}\frac{\partial v}{\partial x}
\end{aligned} \qquad (2)$$

where $\sigma_{ii}(x, z)$ and $\tau_{ij}(x, z)$, $i, j=x, y, z$, are the normal and shear stress components, respectively, and C_{ij}, $i, j=1, 2, \cdots, 6$, are the elastic stiffness constants which take on the different values for the upper and lower orthotropic materials.

In the absence of body forces, the displacement equilibrium equations are expressed as

$$C_{11}\frac{\partial^2 u}{\partial x^2}+C_{55}\frac{\partial^2 u}{\partial z^2}+(C_{13}+C_{55})\frac{\partial^2 w}{\partial x\partial z}=0$$
$$(C_{13}+C_{55})\frac{\partial^2 u}{\partial x\partial z}+C_{55}\frac{\partial^2 w}{\partial x^2}+C_{33}\frac{\partial^2 w}{\partial z^2}=0$$
$$C_{66}\frac{\partial^2 v}{\partial x^2}+C_{44}\frac{\partial^2 v}{\partial z^2}=0 \tag{3}$$

It is seen from the foregoing basic equations that the in-plane deformation, u and w, and the anti-plane deformation, v, are decoupled from each other. In what follows, however, a general solution procedure is provided which uniformly enables the analysis of both the in-plane and anti-plane crack problems in a simultaneous manner.

2.2 Boundary and Interface Conditions

By dividing the interlayer into two regions above and below the cracked plane (Fig. 1), the laminate is modeled as a 4-layer medium. The upper/lower half-space is labelled as the first/fourth layer, while the upper/lower region of the interlayer is labelled as the second/third layer.

The condition of displacement continuity at the perfectly bonded layer interfaces and that of traction equilibrium are to be satisfied such that

$$u_k^-=u_{k+1}^+,\ v_k^-=v_{k+1}^+,\ w_k^-=w_{k+1}^+$$
$$;|x|<\infty,\ k=1,3$$
$$(\sigma_{zz})_k^-=(\sigma_{zz})_{k+1}^+,\ (\tau_{xz})_k^-=(\tau_{xz})_{k+1}^+,$$
$$(\tau_{yz})_k^-=(\tau_{yz})_{k+1}^+;|x|<\infty,\ k=1,2,3 \tag{4}$$

while the regularity conditions at infinity are imposed as

$$(\sigma_{zz})_1^+=0,\ (\tau_{xz})_1^+=0,\ (\tau_{yz})_1^+=0,$$
$$(\sigma_{zz})_4^-=0,\ (\tau_{xz})_4^-=0,\ (\tau_{yz})_4^-=0$$
$$;\sqrt{x^2+z^2}\to\infty \tag{5}$$

where the subscript k or $k+1$ denotes the layer number and the superscript $+/-$ indicates the layer upper/lower surface.

The mixed boundary conditions on the plane containing the crack (the interface between the second and third layers) are expressed as

$$u_2^-=u_3^+,\ v_2^-=v_3^+,\ w_2^-=w_3^+$$
$$;a<|x|<\infty$$
$$(\sigma_{zz})_3^+=p_1(x),\ (\tau_{xz})_3^+=p_2(x),\ (\tau_{yz})_3^+=p_3(x)$$
$$;|x|<a \tag{6}$$

where $p_j(x)$, $j=1, 2, 3$, are functions describing the applied crack surface tractions.

By defining a set of auxiliary functions as

$$\psi_1(x)=\frac{\partial}{\partial x}(w_2^- - w_3^+)$$
$$\psi_2(x)=\frac{\partial}{\partial x}(u_2^- - u_3^+)$$
$$\psi_3(x)=\frac{\partial}{\partial x}(v_2^- - v_3^+)$$
$$;|x|<\infty \tag{7}$$

the mixed conditions in Eqs. (6) can now be written as a set of three homogeneous conditions in terms of the auxiliary functions, subjected to the restrictions to ensure the continuity and single-valuedness of displacements outside the crack surface:

$$\psi_k(x)=0$$
$$;a<|x|<\infty$$
$$\int_{-a}^{a}\psi_k(x)dx=0$$
$$;k=1,2,3 \tag{8}$$

2.3 General Solutions

By employing the Fourier integral transform technique, the governing equations (3) are readily solved to yield the general solutions for the displacement components of orthotropic half-spaces satisfying Eqs. (5) such that

$$u_k=\frac{1}{2\pi}\int_{-\infty}^{\infty}\sum_{j=1}^{2}F_{kj}e^{(-1)^k|s|\lambda_{kj}z-isx}ds,$$
$$w_k=\frac{(-1)^k}{2\pi}\int_{-\infty}^{\infty}\sum_{j=1}^{2}iF_{kj}R_{kj}e^{(-1)^k|s|\lambda_{kj}z-isx}ds,$$
$$v_k=\frac{1}{2\pi}\int_{-\infty}^{\infty}F_{k3}e^{(-1)^k|s|\lambda_{k0}z-isx}ds$$
$$;k=1,4 \tag{9}$$

where s is the transform variable, $F_{kj}(s)$, $k=1, 4$, $j=1, 2, 3$, are the unknowns to be evaluated, $\lambda_{k0}=(C_{66}^{(k)}/C_{44}^{(k)})^{1/2}$, and λ_{kj}, $k=1, 4$, $j=1, 2$, are positive roots of the characteristic equation:

$$C_{35}^{(k)}C_{55}^{(k)}\lambda_k^4+[(C_{13}^{(k)}+C_{55}^{(k)})^2-C_{11}^{(k)}C_{33}^{(k)}$$
$$-(C_{55}^{(k)})^2]\lambda_k^2+C_{11}^{(k)}C_{55}^{(k)}=0;k=1,4 \tag{10}$$

and R_{kj}, $k=1, 4$, $j=1, 2$, are the material constants

$$R_{kj}=\frac{C_{11}^{(k)}-C_{55}^{(k)}\lambda_{kj}^2}{(C_{13}^{(k)}+C_{55}^{(k)})\lambda_{kj}} \tag{11}$$

From Eqs. (2) and (9), the general solutions for the traction components are obtained as

$$(\sigma_{zz})_k=\frac{1}{2\pi}\int_{-\infty}^{\infty}\sum_{j=1}^{2} i(|s|C_{33}^{(k)}\lambda_{kj}R_{kj}-sC_{13}^{(k)})F_{kj}\, e^{(-1)^k|s|\lambda_{kj}z-isx}ds,$$

$$(\tau_{xz})_k=\frac{(-1)^k}{2\pi}\int_{-\infty}^{\infty}\sum_{j=1}^{2} C_{55}^{(k)}(sR_{kj}+|s|\lambda_{kj})F_{kj}\, e^{(-1)^k|s|\lambda_{kj}z-isx}ds,$$

$$(\tau_{yz})_k=\frac{(-1)^k}{2\pi}\int_{-\infty}^{\infty}|s|\lambda_{ko}C_{44}^{(k)}F_{k3}\, e^{(-1)^k|s|\lambda_{ko}z-isx}ds \quad ; k=1, 4 \tag{12}$$

For the matrix interlayer having isotropic properties, there are only two independent elastic constants such that $C_{11}=C_{22}=C_{33}=2\mu_m(1-\nu_m)/(1-2\nu_m)$, $C_{12}=C_{13}=C_{23}=2\mu_m\nu_m/(1-2\nu_m)$, and $C_{44}=C_{55}=C_{66}=\mu_m=E_m/2(\nu_m+1)$ where μ_m, ν_m, and E_m are shear modulus, Poisson's ratio, and Young's modulus of the matrix phase of fiber composites, respectively. The roots of the characteristic equation (10) then become repeated and equal to unity, with the general expressions of displacements and tractions for this special case given as (Choi and Thangjitham, 1991a)

$$u_k=\frac{1}{2\pi}\int_{-\infty}^{\infty}[(A_{k1}+zA_{k2})\cosh sz+(B_{k1}+zB_{k2})\sinh sz]e^{-isx}ds,$$

$$w_k=\frac{1}{2\pi}\int_{-\infty}^{\infty} i\left[\left(A_{k1}+zA_{k2}-\frac{R_m}{s}B_{k2}\right)\sinh sz+\left(B_{k1}+zB_{k2}-\frac{R_m}{s}A_{k2}\right)\cosh sz\right]e^{-isx}ds,$$

$$v_k=\frac{1}{2\pi}\int_{-\infty}^{\infty}(A_{k3}\cosh sz+B_{k3}\sinh sz)e^{-isx}ds \quad ; k=2,3 \tag{13a}$$

$$(\sigma_{zz})_k=\frac{\mu_m}{2\pi}\int_{-\infty}^{\infty} i\{[2s(A_{k1}+zA_{k2})-(R_m+1)B_{k2}]\cosh sz+[2s(B_{k1}+zB_{k2})-(R_m+1)A_{k2}]\sinh sz\}e^{-isx}ds)$$

$$(\tau_{xz})_k=\frac{\mu_m}{2\pi}\int_{-\infty}^{\infty}\{[2s(B_{k1}+zB_{k2})+(1-R_m)A_{k2}]\cosh sz+[2s(A_{k1}+zA_{k2})+(1-R_m)B_{k2}]\sinh sz\}e^{-isx}ds$$

$$(\tau_{yz})_k=\frac{\mu_m}{2\pi}\int_{-\infty}^{\infty}s(A_{k3}\sinh sz+B_{k3}\cosh sz)e^{-isx}ds \quad ; k=2, 3 \tag{13b}$$

where $A_{kj}(s)$ and $B_{kj}(s)$, $k=2, 3$, $j=1, 2, 3$, are the unknowns to be evaluated and $R_m=3-4\nu_m$.

2.4 Stiffness Matrix Formulation

For the entire 4-layer medium, a total of eighteen unknowns exist (three unknowns F_{kj}, $k=1, 4$, $j=1, 2, 3$, for each half-space and six unknowns A_{kj} and B_{kj}, $k=2, 3$, $j=1, 2, 3$, for each region of the interlayer), yet to be evaluated by applying Eqs. (4) and (7). As an efficient approach to accomplishing this intractable task, the stiffness matrix formulation (Choi and Thangjitham, 1991a,b) is extended to the analysis of the current crack problem.

The following quantities are then introduced as

$$\bar{\boldsymbol{d}}_k=[-i\bar{w}_k\ \bar{u}_k\ \bar{v}_k]^T, \tag{14a}$$

$$\bar{\boldsymbol{\sigma}}_k=[-i(\bar{\sigma}_{zz})_k\ (\bar{\tau}_{xz})_k\ (\bar{\tau}_{yz})_k]^T \tag{14b}$$

where $\bar{\boldsymbol{d}}_k(s, z)$ and $\bar{\boldsymbol{\sigma}}_k(s, z)$ are vectors for the displacements and tractions of the kth layer, respectively, in which overbars denote quantities in the Fourier transformed domain (s, z).

The tractions $\bar{\boldsymbol{\sigma}}_k^{\pm}(s)$ at the upper(+)/lower(−) surface of each layer can be expressed in terms of the corresponding displacements $\bar{\boldsymbol{d}}_k^{\pm}(s)$ such that

$$-\bar{\boldsymbol{\sigma}}_1^-=\boldsymbol{K}_{22}^{(1)}\bar{\boldsymbol{d}}_1^-$$

$$\begin{Bmatrix}\bar{\boldsymbol{\sigma}}_k^+\\ -\bar{\boldsymbol{\sigma}}_k^-\end{Bmatrix}=\begin{bmatrix}\boldsymbol{K}_{11}^{(k)} & \boldsymbol{K}_{12}^{(k)}\\ \boldsymbol{K}_{21}^{(k)} & \boldsymbol{K}_{22}^{(k)}\end{bmatrix}\begin{Bmatrix}\bar{\boldsymbol{d}}_k^+\\ \bar{\boldsymbol{d}}_k^-\end{Bmatrix}\ ; k=2, 3$$

$$\bar{\boldsymbol{\sigma}}_4^+=\boldsymbol{K}_{11}^{(4)}\bar{\boldsymbol{d}}_4^+ \tag{15}$$

where $\boldsymbol{K}_{ii}^{(k)}(s)$, $i=1, 2$, $k=1, 4$, are 3×3 symmetric local stiffness matrices for the orthotropic half-spaces and $\boldsymbol{K}_{ij}^{(k)}(s)$, $i, j=1, 2$, $k=2, 3$, are 3×3 submatrices of the 6×6 real and symmetric local stiffness matrices for the matrix interlayer (Appendix), together with the following asymptotic behavior for large values of $|s|$:

$$\lim_{|s|\to\infty}\frac{1}{s}\boldsymbol{K}_{ij}^{(k)}(s)=\begin{cases}\boldsymbol{K}_{ii^\infty}^{(k)}\ ; i=j\\ 0\ \ ; i\neq j\end{cases} \tag{16}$$

in which $\boldsymbol{K}_{ii^\infty}^{(k)}$, $i=1, 2$, denotes 3×3 symmetric submatrices containing nonzero limiting values.

By defining $\bar{\boldsymbol{\sigma}}_k(s)=\bar{\boldsymbol{d}}_k^-(s)=\bar{\boldsymbol{d}}_{k+1}^+(s)$, $k=1, 3$, as vectors for the interfacial displacements common to the perfectly bonded layer interfaces, the traction equilibrium on the cracked plane can be written as

$$\boldsymbol{K}_{21}^{(2)}\bar{\boldsymbol{\delta}}_1+\boldsymbol{K}_{22}^{(2)}\bar{\boldsymbol{d}}_2^-+\boldsymbol{K}_{11}^{(3)}\bar{\boldsymbol{d}}_3^++\boldsymbol{K}_{12}^{(3)}\bar{\boldsymbol{\delta}}_3=0 \tag{17}$$

where from Eqs. (7), (8a) and (14a), the vectors

$\bar{d}_2^-(s)$ and $\bar{d}_3^+(s)$ for the transformed crack surface displacements are related to each other such that

$$\Delta\bar{d}(s)\equiv\bar{d}_2^- - \bar{d}_3^+ = \frac{i}{s}\int_{-a}^{a}\Psi(t)e^{ist}dt \quad (18)$$

in which the vector

$$\Psi=[-i\psi_1 \ \psi_2 \ \psi_3]^T \quad (19)$$

Upon noting that both vectors $\bar{d}_2^-(s)$ and $\bar{d}_3^+(s)$ define the common interfacial displacements $\bar{\delta}_2(s)$ for an otherwise uncracked medium and the additional deformation due to crack extension, from Eqs. (17) and (18) in conjunction with the asymptotic properties in Eq. (16), these vectors can be decomposed as

$$\begin{aligned}\bar{d}_2^- &= \bar{\delta}_2 + L_\infty K_{11^\infty}^{(3)}\Delta\bar{d},\\ \bar{d}_3^+ &= \bar{\delta}_2 - L_\infty K_{22^\infty}^{(2)}\Delta\bar{d}\end{aligned} \quad (20)$$

where L_∞ is a 3×3 symmetric constant matrix written as

$$L_\infty=[K_{11^\infty}^{(3)}+K_{22^\infty}^{(2)}]^{-1} \quad (21)$$

Through the successive applications of Eq. (4) to the layer local stiffness matrix equations (15) and using Eq. (20), a global stiffness matrix equation for the composite laminate containing an interlaminar crack is constructed as

$$\begin{bmatrix} K_{22}^{(1)}+K_{11}^{(2)} & K_{12}^{(2)} & 0\\ K_{21}^{(2)} & K_{22}^{(2)}+K_{11}^{(3)} & K_{12}^{(3)}\\ 0 & K_{21}^{(3)} & K_{22}^{(3)}+K_{11}^{(4)}\end{bmatrix}\begin{Bmatrix}\bar{\delta}_1\\ \bar{\delta}_2\\ \bar{\delta}_3\end{Bmatrix}=\begin{Bmatrix}f_1\\ f_2\\ f_3\end{Bmatrix} \quad (22)$$

where $f_i(s)$, $i=1, 2, 3$, are vectors of length three expressed as

$$\begin{aligned} f_1 &= -K_{12}^{(2)}L_\infty K_{11^\infty}^{(3)}\Delta\bar{d}\\ f_2 &= (K_{11}^{(3)}L_\infty K_{22^\infty}^{(2)} - K_{22}^{(2)}L_\infty K_{11^\infty}^{(3)})\Delta\bar{d}\\ f_3 &= -K_{21}^{(3)}L_\infty K_{22^\infty}^{(2)}\Delta\bar{d}\end{aligned} \quad (23)$$

In matrix notation, the above system of equations is written as

$$K\bar{\delta}=f \quad (24)$$

where $K(s)$ is a 9×9 banded and symmetric global stiffness matrix, $\bar{\delta}(s)$ is a vector of length nine for the unknown common interfacial displacements, and $\bar{f}(s)$ is a vector of length nine containing the geometric and material properties of the interlayer and the crack surface displacements.

2.5 Integral Equations

After substituting the crack surface displacement vectors in Eq. (20) into Eq. (15) and using the values of $\bar{\delta}(s)$ from Eq. (24), the tractions $\sigma_3^+(x)$ acting on plane containing the crack can be obtained by taking the inverse Fourier transform such that

$$\sigma_3^+(x)=\frac{i}{2\pi}\int_{-a}^{a}\left[\int_{-\infty}^{\infty}\frac{1}{s}M(s)e^{is(t-x)}ds\right]\Psi(t)dt \quad ;|x|<\infty \quad (25)$$

where $M(s)$ is a 3×3 matrix written as

$$M=-K_{11}^{(3)}L_\infty K_{22^\infty}^{(2)}+K_{11}^{(3)}H_1+K_{12}^{(3)}H_2 \quad (26)$$

in which $H_n(s), n=1,2$, are 3×3 matrices expressed as

$$\begin{aligned} H_n=&-L_{(1+n)1}K_{12}^{(2)}L_\infty K_{11^\infty}^{(3)}\\ &+L_{(1+n)2}(K_{11}^{(3)}L_\infty K_{22^\infty}^{(2)}-K_{22}^{(2)}L_\infty K_{11^\infty}^{(3)})\\ &+L_{(1+n)3}(K_{21}^{(3)}L_\infty K_{22^\infty}^{(2)}\ ;\ n=1,\ 2\end{aligned} \quad (27)$$

where $L_{ij}(s)$, $i, j=1, 2, 3$, are 3×3 submatrices of $L(s)\equiv K^{-1}(s)$.

It can be further shown from Eqs. (16),(26), and (27) that the matrices $H_n(s)$, $n=1, 2$, and $M(s)$ have the following asymptotic behavior

$$\begin{aligned}\lim_{|s|\to\infty}\frac{1}{s}H_n(s)&=0\ ;\ n=1,\ 2\\ \lim_{|s|\to\infty}\frac{1}{s}M(s)&\equiv\lim_{|s|\to\infty}\frac{1}{s}\begin{bmatrix}m_{11} & m_{12} & 0\\ m_{21} & m_{22} & 0\\ 0 & 0 & m_{33}\end{bmatrix}\\ &=-\frac{s}{|s|}\begin{bmatrix}m_{11^\infty} & 0 & 0\\ 0 & m_{22^\infty} & 0\\ 0 & 0 & m_{33^\infty}\end{bmatrix}\end{aligned} \quad (28)$$

where on the ground that both the second and third layers belong to the same matrix interlayer, the constants m_{ll^∞}, $l=1, 2, 3$, are obtained as

$$m_{11^\infty}=m_{22^\infty}=\frac{\mu_m}{2(1-\nu_m)},\ m_{33^\infty}=\frac{\mu_m}{2} \quad (29)$$

The foregoing results make it clear that the singularities of the integral equations (25) are attributable to the asymptotic values of the integrand $s^{-1}M(s)$ as $|s|$ approaches infinity. In consequence, separation of the singular part in Eq. (25) can lend itself to a system of Cauchy-type singular integral equations of the first kind such that

$$\frac{\mu_m}{2\pi(1-\nu_m)}\int_{-a}^{a}\frac{\psi_1(t)}{t-x}dt + \int_{-a}^{a}\sum_{n=1}^{2}k_{1n}(x,\ t)\psi_n(t)dt=p_1(x),$$

$$\frac{\mu_m}{2\pi(1-\nu_m)}\int_{-a}^{a}\frac{\psi_2(t)}{t-x}dt + \int_{-a}^{a}\sum_{n=1}^{2}k_{2n}(x,\ t)\psi_n(t)dt=p_2(x),$$

$$\frac{\mu_m}{2\pi}\int_{-a}^{a}\frac{\psi_3(t)}{t-x}dt+\int_{-a}^{a}k_{33}(x,\ t)\psi_3(t)dt = p_3(x)\ ;\ |x|<a \tag{30}$$

where $k_{ij}(x,\ t)$, $i,\ j=1,\ 2,\ 3$, are referred to as the bounded Fredholm kernels written as

$$k_{ij}(x,\ t)=-\frac{1}{\pi}\int_0^{\infty}\left[\frac{1}{s}m_{ij}(s)+m_{ij}^{\infty}\right]\sin s(t-x)ds$$
$$;(i,\ j)=(1,\ 1),\ (2,\ 2),\ (3,\ 3)$$

$$k_{12}(x,\ t)=-\frac{1}{\pi}\int_0^{\infty}\frac{1}{s}m_{12}(s)\cos s(t-x)ds$$

$$k_{21}(x,\ t)=\frac{1}{\pi}\int_0^{\infty}\frac{1}{s}m_{21}(s)\cos s(t-x)ds \tag{31}$$

The singular integral equations obtained as above demonstrate that there is no coupling between Eqs. (30a, b) and Eq. (30c). This indicates that the in-plane and anti-plane responses of the interlaminar crack in the orthotropic bimaterials are independent of each other.

Via the existence of dominant Cauchy-type singular kernels in Eqs. (30), the singular nature of the auxiliary functions, ψ_k, $k=1,\ 2,\ 3$, is characterized by the fundamental function of the integral equations (Muskhelishvili, 1953). Such a function, in this case, corresponds to the weight function of the Chebyshev polynomial of the first kind (Erdogan, 1977). To preserve the correct nature of singularities of the problem, the solutions to the integral equations in the normalized intervals, $\xi=x/a$ and $\tau=t/a$, can then be expressed as

$$\psi_k(\tau)=\frac{1}{\sqrt{1-\tau^2}}\sum_{n=1}^{\infty}c_{kn}T_n(\tau)$$
$$;\ k=1,2,3,\ |\tau|<1 \tag{32}$$

where c_{kn}, $k=1,\ 2,\ 3$, and $n\geq 1$, are the unknown constants yet to be evaluated and $T_n(\tau)$ is the Chebyshev polynomial of the first kind of order n, and $1/(1-\tau^2)^{1/2}$ is the corresponding weight function. To be noted herein is that the compatibility condition in Eq. (8b) is identically satisfied by the above series expansion.

Upon substituting Eq. (32) into Eqs. (30) and using the integral formula (Abramowitz and Stegun,1965)

$$\frac{1}{\pi}\int_{-1}^{1}\frac{T_n(\tau)d\tau}{\sqrt{1-\tau^2}(\tau-\xi)}=U_{n-1}(\xi)$$
$$;\ n\geq 1,\ |\xi|<1 \tag{33}$$

the singularities of the integral equations are removed such that

$$\frac{\mu_m}{2(1-\nu_m)}\sum_{n=1}^{\infty}c_{ln}U_{n-1}(\xi) + \sum_{n=1}^{\infty}\sum_{m=1}^{2}H_n^{lm}(\xi)c_{mn}=p_l(\xi)$$
$$;\ l=1,\ 2,\ |\xi|<1$$

$$\frac{\mu_m}{2}\sum_{n=1}^{\infty}c_{3n}U_{n-1}(\xi)+\sum_{n=1}^{\infty}H_n^{33}(\xi)c_{3n}=p_3(\xi)$$
$$;\ |\xi|<1 \tag{34}$$

where $U_n(\tau)$ is the Chebyshev polynomial of the second kind and $H_n^{lm}(\xi)$ is defined as

$$H_n^{lm}(\xi)=a\int_{-1}^{1}\frac{k_{lm}(\xi,\ \tau)T_n(\tau)}{\sqrt{1-\tau^2}}d\tau \tag{35}$$

To recast the above functional equations (34) into a solvable form, the following orthogonal relation for $U_n(\tau)$ is utilized in the sense of the weighted residual method (Abramowitz and Stegun, 1965)

$$\frac{2}{\pi}\int_{-1}^{1}U_k(\tau)U_n(\tau)\sqrt{1-\tau^2}d\tau=\begin{cases}0\ ;\ k\neq n\\ 1\ ;\ k=n\end{cases} \tag{36}$$

and a system of linear algebraic equations for c_{kn} is obtained as

$$\frac{\pi\mu_m}{4(1-\nu_m)}c_{lk}+\sum_{n=1}^{\infty}\sum_{m=1}^{2}Y_{kn}^{lm}c_{mn}=\delta_k^l$$
$$;\ l=1,\ 2,\ k=1,\ 2,\ 3,\ \cdots,$$

$$\frac{\pi\mu_m}{4}c_{3k}+\sum_{n=1}^{\infty}Y_{kn}^{33}c_{3n}=\delta_k^3$$
$$;\ k=1,\ 2,\ 3,\ \cdots, \tag{37}$$

where the constants Y_{kn}^{lm} and δ_k^l are expressed as

$$Y_{kn}^{lm}=\int_{-1}^{1}H_n^{lm}(\xi)U_{k-1}(\xi)\sqrt{1-\xi^2}d\xi$$

$$\delta_k^l=\int_{-1}^{1}p_l(\xi)U_{k-1}(\xi)\sqrt{1-\xi^2}d\xi \tag{38}$$

The series in Eq. (32) is truncated, in practice, after the first N terms leading to a system of $3N$

simultaneous equations for c_{kn}, $k=1$, 2, 3, and $1 \leq n \leq N$ in Eq. (37). This number N must be large enough for the solution to be within a specified degree of accuracy. Upon solving the truncated version of Eq. (37), the dominant singular terms of crack-tip tractions can thus be obtained from Eq. (25) in terms of the solutions to the integral equations as

$$(\sigma_{zz})_3^+(\xi)=\frac{\mu_m}{2(1-\nu_m)}\sum_{n=1}^{N} c_{1n}S_n(\xi)+0(1),$$

$$(\tau_{xz})_3^+(\xi)=\frac{\mu_m}{2(1-\nu_m)}\sum_{n=1}^{N} c_{2n}S_n(\xi)+0(1),$$

$$(\tau_{yz})_3^+(\xi)=\frac{\mu_m}{2}\sum_{n=1}^{N} c_{3n}S_n(\xi)+0(1)$$

$$; |\xi|>1 \tag{39}$$

where $O(\cdot)$ denotes the higher order terms and the function $S_n(\xi)$ is written as

$$S_n(\xi)=-\frac{[\xi-\mathrm{sgn}(\xi)\sqrt{\xi^2-1}]^n}{\mathrm{sgn}(\xi)\sqrt{\xi^2-1}}$$

$$; n\geq 1,\ |\xi|>1 \tag{40}$$

The stress intensity factors at the right-hand side crack tip can therefore be evaluated from the solution structure obtained for the crack-tip tractions such that

$$K_{\mathrm{I}}\equiv\lim_{\xi\to 1^+}\sqrt{\xi^2-1}\,(\sigma_{zz})_3^+(\xi)=-\frac{\mu_m}{2(1-\nu_m)}\sum_{n=1}^{N} c_{1n}$$

$$K_{\mathrm{II}}\equiv\lim_{\xi\to 1^+}\sqrt{\xi^2-1}\,(\tau_{xz})_3^+(\xi)=-\frac{\mu_m}{2(1-\nu_m)}\sum_{n=1}^{N} c_{2n}$$

$$K_{\mathrm{III}}\equiv\lim_{\xi\to 1^+}\sqrt{\xi^2-1}\,(\tau_{yz})_3^+(\xi)=-\frac{\mu_m}{2}\sum_{n=1}^{N} c_{3n} \tag{41}$$

where K_{I}, K_{II}, and K_{III} are mode I, II, and III stress intensity factors, respectively, and at the left-hand side crack-tip, the negative sign is replaced by $(-1)^n$.

3. Results and Discussion

For the purpose of numerical illustrations, a fiber-reinforced composite material with the following fiber (T300 graphite) and matrix (epoxy) properties is considered (Chamis, 1984)

$E_{f1}=220.6$ GPa, $\nu_{f1}=0.2$, $\mu_{f1}=8.9$ GPa
$E_{f2}=13.8$ GPa, $\nu_{f2}=0.25$, $\mu_{f1}=4.8$ GPa
$E_m=3.45$ GPa, $\nu_m=0.35$, $\mu_m=1.28$ GPa

where the subscript m refers to the matrix phase, while the subscripts $f1$ and $f2$ denote the longitudinal and transverse directions of the fiber phase, respectively.

By regarding the fibrous composite as effectively homogeneous and orthotropic, the corresponding elastic stiffness constants $C_{ij}^{(k)}$, $k=1$, 4, are evaluated via the composite micromechanics equations (Chamis, 1984). For the fiber volume fraction of $V_f=0.5$, the values of stiffness constants for the upper ($\theta=0°$) and lower ($\theta=90°$) orthotropic half-spaces are obtained as

upper half-space
$C_{11}^{(1)}=114$ GPa, $C_{22}^{(1)}=C_{33}^{(1)}=8.7$ GPa
$C_{12}^{(1)}=C_{13}^{(1)}=3.3$ GPa, $C_{23}^{(1)}=3.4$ GPa
$C_{44}^{(1)}=2.7$ GPa, $C_{55}^{(1)}=C_{66}^{(1)}=3.2$ GPa
lower half-space
$C_{11}^{(4)}=C_{33}^{(4)}=8.7$ GPa, $C_{22}^{(4)}=114$ GPa
$C_{12}^{(4)}=C_{23}^{(4)}=3.3$ GPa, $C_{13}^{(4)}=3.4$ GPa
$C_{44}^{(4)}=C_{66}^{(4)}=3.2$ GPa, $C_{55}^{(4)}=2.7$ GPa

Without loss in generality, the following modes of loadings are prescribed in which the crack surface loading functions $p_j(x)$, $j=1$, 2, 3, in Eq. (6b) are given as:

For the in-plane normal (mode I) loading

$$p_1(x)=-\sigma_o,\ p_2(x)=0,\ p_3(x)=0\,;\ |x|<a$$

For the in-plane shear (mode II) loading

$$p_1(x)=0,\ p_2(x)=-\tau_o,\ p_3(x)=0\,;\ |x|<a$$

For the anti-plane shear (mode III) loading

$$p_1(x)=0,\ p_2(x)=0,\ p_3(x)=-s_o\,;\ |x|<a$$

where σ_o, τ_o, and s_o are, respectively, the magnitudes of in-plane normal, in-plane shear, and anti-plane shear tractions uniformly applied on the crack surface.

Depending on the loading conditions, the series in Eq. (32) can either be expanded in terms of odd or even numbers. Specifically, under mode I loading, the Chebyshev polynomials for ψ_1 and ψ_2 are to be expanded in terms of odd and even numbers, respectively, while the reverse is true under mode II loading. For the case of mode III loading, the polynomial for ψ_3 is to be expanded in terms of odd numbers. In this manner, a twelve-term expansion of the Chebyshev polynomials is found to suffice in obtaining the solution with a required degree of accuracy, together with the numerical evaluation of related integrals based on

the Gauss-Chebyshev and Gauss-Legendre quadrature formulas (Abramowitz and Stegun, 1965). It is noted that, in the present discussion, the stress intensity factors are evaluated at the right-hand side crack tip and for $V_f=0.5$ unless otherwise stated.

With the interlaminar crack located at the midplane of the interlayer such that $h_1/h_2=1$, the values of major stress intensity factors, K_i, $i=$I, II, III, are shown in Fig. 2 as a function of relative crack size h/a, to be directly identified with the modes of applied loadings. In this figure, the normalized stress intensity factors are observed to increase monotonically in proportion to the ratio h/a but remain below the upper bound of unity. This may be indicative of improved load-carrying capacity of the fibrous laminated composite against fracture in comparison with that of a conventional homogeneous material of the same extent.

Because of the mismatches of layer material properties, the mixed-mode behavior is predicted in Fig. 3 by the simultaneous occurrence of coupling stress intensity factors K_{II} and K_I under mode I and II loadings, respectively. Such values of K_{II} and K_I are, however, becoming insignificant as h/a increases. In particular, a crack-tip state of compressive singular normal stresses is depicted under the in-plane shear loading, as indicated by the negative values of K_I. Owing to the antisymmetry of mode II loading, the K_I at the left-hand side crack tip is equal in magnitude but opposite in sign, implying the partial crack closure at one of the crack tips. Although the initial assumption of a frictionless, open crack model may thus be violated, in the light of general loading conditions where there exists a sufficiently large component of tensile loading, such negative solutions for K_I can have a meaning provided that the superimposed values of K_I at both the crack tips become positive. To be noted is that under mode III loading, only the values of K_{III} are induced as the major crack-tip response and there occurs no mixed-mode stress intensification.

The effect of relative crack location, $h_1/2h$, is

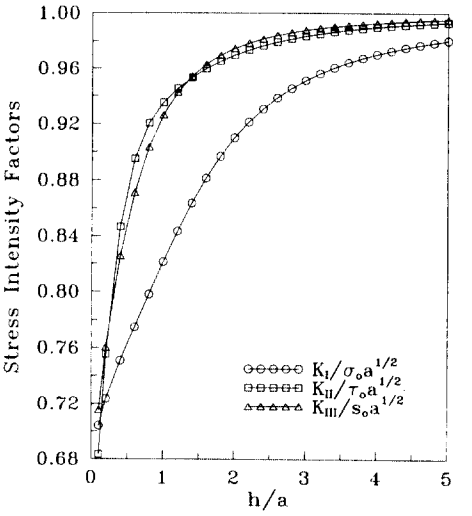

Fig. 2 Variation of major stress intensity factors as a function of relative crack size h/a for $h_1/h_2=1$ and $V_f=0.5$

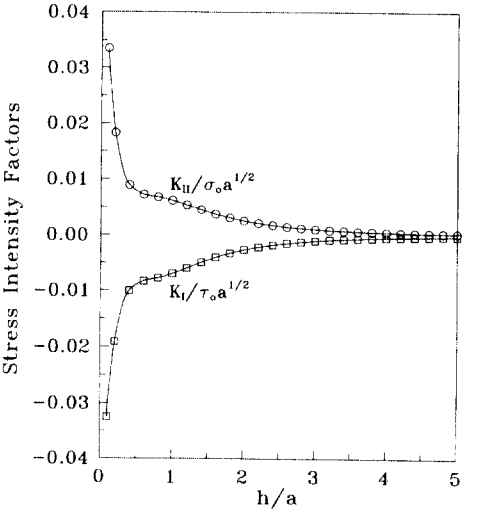

Fig. 3 Variation of coupling stress intensity factors as a function of relative crack size h/a for $h_1/h_2=1$ and $V_f=0.5$

next considered. Specific results are obtained for $h/a=1$ and plotted in Figs. 4 and 5 for the major and coupling stress intensity factors, respectively. Figure 4 illustrates that the values of K_I experience slight and monotonic increases as $h_1/2h$ becomes relatively large. On the other hand, the

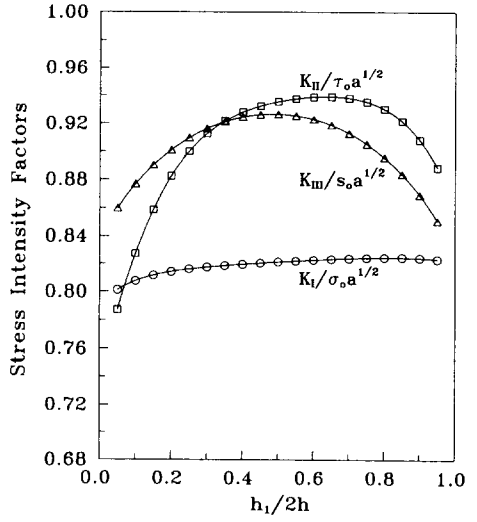

Fig. 4 Variation of major stress intensity factors as a function of relative crack location $h_1/2h$ for $h/a=1$ and $V_f=0.5$

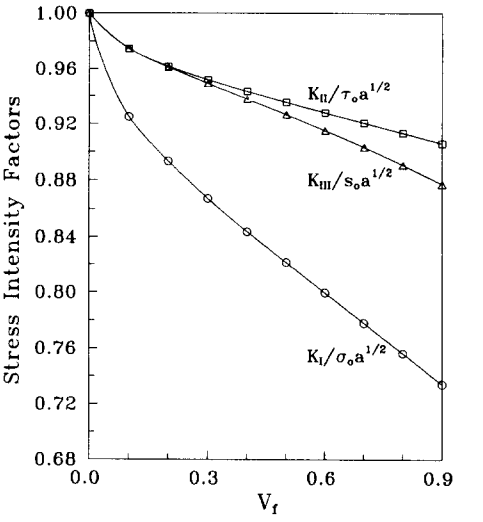

Fig. 6 Variation of major stress intensity factors as a function of fiber volume fraction V_f for $h/a=1$ and $h_1/h_2=1$

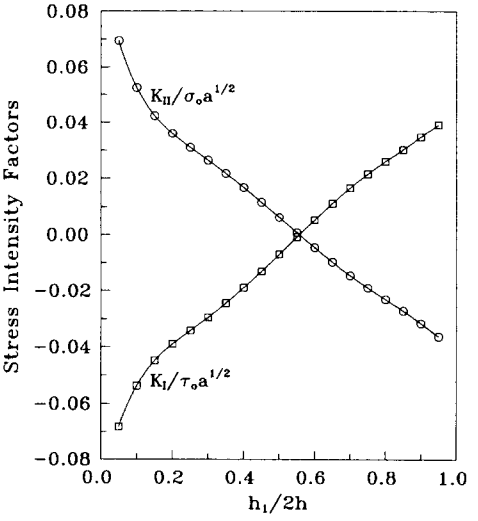

Fig. 5 Variation of coupling stress intensity factors as a function of relative crack location $h_1/2h$ for $h/a=1$ and $V_f=0.5$

values of K_{II} and K_{III} are influenced to a much greater extent by $h_1/2h$ when compared with those of K_I. In Fig. 5, it is shown that the signs of coupling stress intensity factors may change with respect to varying crack locations within the interlayer. Of interest in this figure is that the mixed-mode behavior appears to vanish when the crack is located around $h_1/2h=0.55$.

It is now worth mentioning that in going to limit $h/a=0$ and $h_1/2h=0$ or 1, the problem reduces to that of bonded dissimilar orthotropic half-spaces containing the crack at the ideal nominal interface. The integral equations describing the in-plane behavior are then changed to those of the second kind (Sun and Manoharan, 1989; Dhaliwal and Saxena, 1990; Hwu, 1993). Because the corresponding nature of crack-tip singularities is oscillatory type and different definitions of stress intensity factors are required, the results for these limiting cases are not provided herein.

For the fixed values of $h/a=1$ and $h_1/h_2=1$, substantial effects of fiber volume fraction V_f on the major stress intensity factors are presented in Fig. 6. Observed in this figure is that increased fiber content from the isotropy of the matrix phase ($V_f=0$) tends to lower the major intensification of crack-tip tractions. The overall increases in fiber composite elastic moduli in parallel with V_f, especially in the fiber direction, are understood to be mainly responsible for such a reduction in the magnitudes of major stress intensity factors. For the case of coupling stress intensity factors as shown in Fig. 7, the reverse trend is

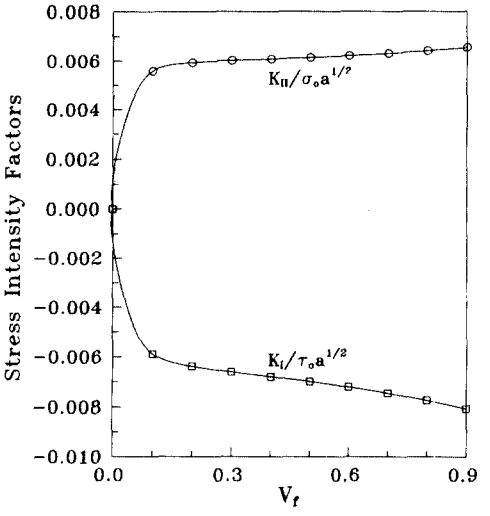

Fig. 7 Variation of coupling stress intensity factors as a function of fiber volume fraction V_f for $h/a=1$ and $h_1/h_2=1$

obtained with respect to V_f. In this case, however, the degree of dependence on V_f appears to be insignificant.

4. Closure

Analytical solutions are presented for the problem of an interlaminar crack in dissimilar orthotropic composite materials, by embedding the crack tips within the matrix interlayer bounded by the orthotropic half-spaces. The stress intensity factors are readily defined from the crack-tip tractions with the standard order of inverse square-root singularities. As a result, under in-plane normal, in-plane shear, and anti-plane shear loading conditions, effects of parameters of physical interest such as the relative crack size, crack location, and fiber volume fraction on the values of major and coupling stress intensity factors are demonstrated.

References

Abramowitz, M. and Stegun, I. A., 1965, *Handbook of Mathematical Functions,* Dover, New York.

Atkinson, C., 1977, "On Stress Singularities and Interfaces in Linear Elastic Fracture Mechanics," *Int. J. Fract.,* Vol. 13, pp. 807~820.

Chamis, C. C., 1984, "Simplified Composite Micromechanics Equations for Hygral, Thermal, and Mechanical Properties," *SAMPE Quarterly,* April, pp. 14~23.

Choi, H. J. and Thangjitham, S., 1991a, "Micro- and Macromechanical Stress and Failure Analyses of Laminated Composites," *Comp. Sci. and Tech.,* Vol. 40, pp. 289~305.

Choi, H. J. and Thangjitham, S., 1991b, "Stress Analysis of Multilayered Anisotropic Elastic Media," *ASME J. Appl. Mech.,* Vol. 58, pp. 382~387.

Comninou, M., 1977, "The Interface Crack," *ASME J. Appl. Mech.,* Vol. 44, pp. 631~636.

Comninou, M., 1990, "An Overview of Interface Cracks," *Eng. Fract. Mech.,* Vol. 37, pp. 197~208.

Delale, F. and Erdogan, F., 1988, "On the Mechanical Modeling of the Interfacial Region in Bonded Half-Plane," *ASME J. Appl. Mech.,* Vol. 55, pp. 317~324.

Dhaliwal, R. S. and Saxena, H. S., 1990, "A Griffith Crack at the Interface of Two Bonded Dissimilar Orthotropic Elastic Half-Planes," *Eng. Fract. Mech.,* Vol. 37, pp. 817~824.

England, A.H., 1965, "A Crack Between Dissimilar Media," *ASME J. Appl. Mech.,* Vol. 32, pp. 400~402.

Erdogan, F., 1977, "Mixed Boundary-value Problems in Mechanics," *Mechanics Today,* vol. 4, pp. 1~86, Nemat-Nasser, S., ed., Pergamon Press.

Erdogan, F. and Gupta, G. D., 1971, "Layered Composites with an Interface Flaw," *Int. J. Solids and Struct.,* Vol. 7, pp. 1089~1107.

Hwu, C., 1993, "Fracture Parameters for the Orthotropic Bimaterial Interface Cracks," *Eng. Fract. Mech.,* Vol. 45, pp. 89~97.

Itou, S., 1986, "Stresses Around an Interface Crack," *Eng. Fract. Mech.,* Vol. 25, pp. 415~420.

Jones, R. M., 1975, *Mechanics of Composite of Materials,* Hemisphere Pub. Corp., New York.

Lekhnitskii, S. G., 1981, *Theory of Elasticity of an Anisotropic Body,* Mir Pub., Moscow.

Muskhelishvili, N. I., 1953, *Singular Integral Equations,* Noordhoff, The Netherlands.

Rice, J. R., 1988, "Elastic Fracture Mechanics Concepts for Interfacial Cracks," *ASME J. Appl. Mech.,* Vol. 55, pp. 98~103.

Sinclair, G.B., 1980, "On the Stress Singularity at an Interface Crack," *Int. J. Fract.,* Vol. 16, pp. 111~119.

Sun, C. T. and Manoharan, M. G., 1989, "Strain Energy Release Rates of an Interfacial Crack Between Two Orthotropic Solids," *J. Comp. Mat.,* Vol. 23, pp. 460~478.

Toya, M., 1992, "On Mode I and Mode II Energy Release Rates of an Interface Crack," *Int. J. Fract.,* Vol. 56, pp. 345~352.

Wang, S. S. and Choi, I., 1983, "The Interface Crack Between Dissimilar Anisotropic Composite Materials," *ASME J. Appl. Mech.,* Vol. 50, pp. 169~178.

Wang, S. S. and Wang H.T., 1979, "Interlaminar Crack Growth in Fiber-Reinforced Composites During Fatigue," *ASME J. Eng. Mat. and Tech.,* Vol. 101, pp. 34~41.

Wu, K. -C. and Chiu, Y. -T., 1991, "Antiplane Shear Interface Cracks in Anisotropic Bimaterials," *ASME J. Appl. Mech.,* Vol. 58, pp. 399~403.

Appendix

The 6x6 local stiffness matrices for the upper/lower region of the matrix interlayer are written as

$$\begin{bmatrix} \boldsymbol{K}_{11}^{(k)} & \boldsymbol{K}_{12}^{(k)} \\ \boldsymbol{K}_{21}^{(k)} & \boldsymbol{K}_{22}^{(k)} \end{bmatrix} = \begin{bmatrix} K_{11}^{(k)} & K_{12}^{(k)} & 0 & K_{14}^{(k)} & K_{15}^{(k)} & 0 \\ K_{12}^{(k)} & K_{22}^{(k)} & 0 & K_{24}^{(k)} & K_{25}^{(k)} & 0 \\ 0 & 0 & K_{33}^{(k)} & 0 & 0 & K_{36}^{(k)} \\ K_{14}^{(k)} & K_{24}^{(k)} & 0 & K_{44}^{(k)} & K_{45}^{(k)} & 0 \\ K_{15}^{(k)} & K_{25}^{(k)} & 0 & K_{45}^{(k)} & K_{55}^{(k)} & 0 \\ 0 & 0 & K_{36}^{(k)} & 0 & 0 & K_{66}^{(k)} \end{bmatrix} ; k=2, 3 \quad \text{(A1)}$$

with the following explicit expressions for the elements $K_{ij}^{(k)}(s)$, $k=2$, 3, given as

$$\begin{aligned} K_{11}^{(k)} &= K_{44}^{(k)} = -\Gamma_k[h_k s^2 + s(3-4\nu_m) \\ &\quad \sinh sh_k \cosh sh_k] \\ K_{12}^{(k)} &= -K_{45}^{(k)} = 2\mu_m s + \Gamma_k' s(3-4\nu_m)\sinh^2 sh_k \\ K_{14}^{(k)} &= \Gamma_k[h_k s^2 \cosh sh_k + s(3-4\nu_m)\sinh sh_k] \\ K_{15}^{(k)} &= -K_{24}^{(k)} = \Gamma_k h_k s^2 \sinh sh_k \\ K_{22}^{(k)} &= K_{55}^{(k)} = \Gamma_k[h_k s^2 - s(3-4\nu_m)\sinh sh_k \cosh sh_k] \\ K_{25}^{(k)} &= \Gamma_k[s(3-4\nu_m)\sinh sh_k - h_k s^2 \cosh sh_k] \\ K_{33}^{(k)} &= K_{66}^{(k)} = \frac{\mu_m s \cosh sh_k}{\sinh sh_k} \\ K_{36}^{(k)} &= -\frac{\mu_m s}{\sinh sh_k} \end{aligned} \quad \text{(A2)}$$

$$\Gamma_k = \frac{4\mu_m(1-\nu_m)}{h_k^2 s^2 - (3-4\nu_m)^2 \sinh^2 sh_k} \quad \text{(A3)}$$

while the 3×3 local stiffness matrices for the upper/lower orthotropic half-space are given as follows, together with the corresponding elements $K_{ij}^{(k)}(s)$, $k=1$, 4, such that

$$\boldsymbol{K}_{ll}^{(k)} = \begin{bmatrix} K_{11}^{(k)} & K_{12}^{(k)} & 0 \\ K_{12}^{(k)} & K_{22}^{(k)} & 0 \\ 0 & 0 & K_{33}^{(k)} \end{bmatrix} ; (k, l)=(1, 2), (4, 1) \quad \text{(A4)}$$

$$\begin{aligned} K_{11}^{(k)} &= \frac{C_{33}^{(k)}}{R_{k1}-R_{k2}} |s|(\lambda_{k1}R_{k1} - \lambda_{k2}R_{k2}) \\ K_{12}^{(k)} &= \frac{(-1)^k}{R_{k1}-R_{k2}}[sC_{33}^{(k)} R_{k1}R_{k2}(\lambda_{k2}-\lambda_{k1})] \\ &\quad -(-1)^k sC_{13}^{(k)} \\ K_{22}^{(k)} &= \frac{C_{55}^{(k)}}{R_{k1}-R_{k2}} |s|(\lambda_{k2}R_{k1} - \lambda_{k1}R_{k2}) \\ K_{33}^{(k)} &= |s|\lambda_{k0} C_{44}^{(k)} \end{aligned} \quad \text{(A5)}$$